



HAL
open science

A new paradigm for gaseous ligand selectivity of hemoproteins highlighted by soluble guanylate cyclase

Gang Wu, Emil Martin, Vladimir Berka, Wen Liu, Elsa Garcin, Ah-Lim Tsai

► To cite this version:

Gang Wu, Emil Martin, Vladimir Berka, Wen Liu, Elsa Garcin, et al.. A new paradigm for gaseous ligand selectivity of hemoproteins highlighted by soluble guanylate cyclase. *Journal of Inorganic Biochemistry*, 2022, 214, 10.1016/j.jinorgbio.2020.111267 . hal-03596344

HAL Id: hal-03596344

<https://hal.science/hal-03596344>

Submitted on 3 Mar 2022

HAL is a multi-disciplinary open access archive for the deposit and dissemination of scientific research documents, whether they are published or not. The documents may come from teaching and research institutions in France or abroad, or from public or private research centers.

L'archive ouverte pluridisciplinaire **HAL**, est destinée au dépôt et à la diffusion de documents scientifiques de niveau recherche, publiés ou non, émanant des établissements d'enseignement et de recherche français ou étrangers, des laboratoires publics ou privés.



HHS Public Access

Author manuscript

J Inorg Biochem. Author manuscript; available in PMC 2022 January 01.

Published in final edited form as:

J Inorg Biochem. 2021 January ; 214: 111267. doi:10.1016/j.jinorgbio.2020.111267.

A new paradigm for gaseous ligand selectivity of hemoproteins highlighted by soluble guanylate cyclase

Gang Wu^{*,#}, Emil Martin^{\$}, Vladimir Berka[#], Wen Liu[,], Elsa D. Garcin^{¶,‡}, Ah-Lim Tsai^{*,#}

[#]:Hematology Division, Department of Internal Medicine, the University of Texas – McGovern Medical School, 6431 Fannin Street, Houston, TX 77030.

^{\$}:Cardiology Division, Department of Internal Medicine, the University of Texas – McGovern Medical School, 1941 East Road, Houston, TX 77054.

[,]:Center for Infectious and Inflammatory Diseases, Texas A&M Institute of Biosciences & Technology, 2121 W Holcombe Blvd., Houston, TX 77030

[¶]:Department of Chemistry and Biochemistry, University of Maryland, Baltimore County, 1000 Hilltop Cir, Baltimore, MD 21250

[‡]:Current address: Laboratoire d'Information Génomique et Structurale, UMR7256, Aix-Marseille Université, Campus de Luminy, 163 Avenue de Luminy, 13288 Marseille (France)

Abstract

Nitric oxide (NO), carbon monoxide (CO), and oxygen (O₂) are important physiological messengers whose concentrations vary in a remarkable range, [NO] typically from nM to several μM while [O₂] reaching to hundreds of μM. One of the machineries evolved in living organisms for gas sensing is sensor hemoproteins whose conformational change upon gas binding triggers downstream response cascades. The recently proposed “sliding scale rule” hypothesis provides a general interpretation for gaseous ligand selectivity of hemoproteins, identifying five factors that govern gaseous ligand selectivity. Hemoproteins have intrinsic selectivity for the three gases due to a neutral proximal histidine ligand while proximal strain of heme and distal steric hindrance indiscriminately adjust the affinity of these three gases for heme. On the other hand, multiple-step NO binding and distal hydrogen bond donor(s) specifically enhance affinity for NO and O₂, respectively. The “sliding scale rule” hypothesis provides clear interpretation for dramatic selectivity for NO over O₂ in soluble guanylate cyclase (sGC) which is an important example of sensor hemoproteins and plays vital roles in a wide range of physiological functions. The “sliding

*Corresponding authors: gang.wu@uth.tmc.edu and ah-lim.tsai@uth.tmc.edu, fax, (713)-500-6812.

Publisher's Disclaimer: This is a PDF file of an unedited manuscript that has been accepted for publication. As a service to our customers we are providing this early version of the manuscript. The manuscript will undergo copyediting, typesetting, and review of the resulting proof before it is published in its final form. Please note that during the production process errors may be discovered which could affect the content, and all legal disclaimers that apply to the journal pertain.

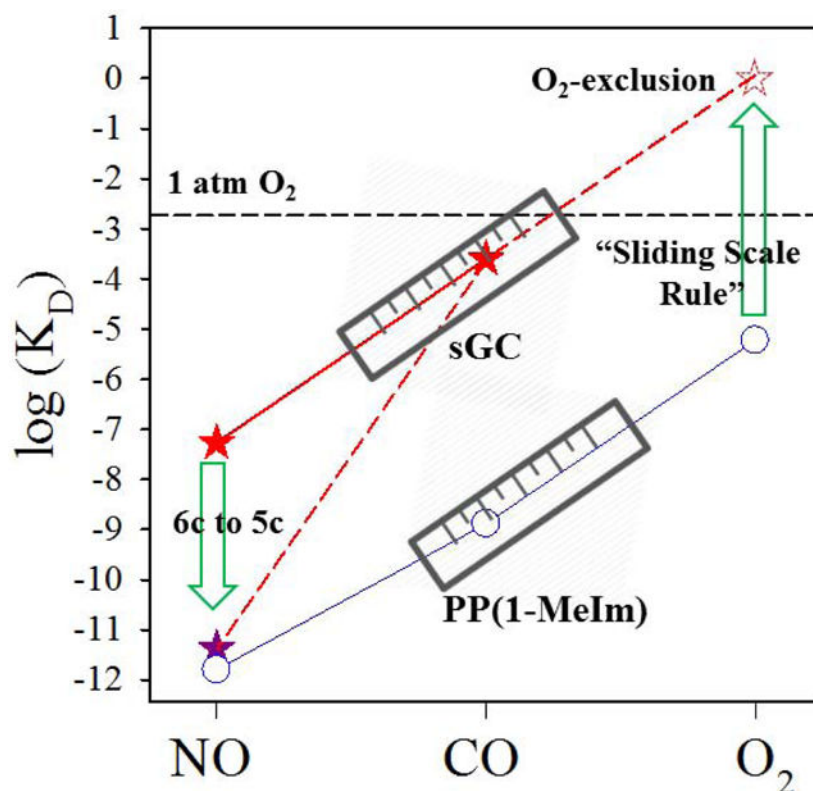
Appendix A. Supplementary Information

Supporting information to this article includes the experimental procedures and results of measuring kinetics and affinity of gaseous ligands for 1) two truncated sGC constructs, *Bt* sGC β₁(1-359) containing the H-NOX, PAS, and partial CC domains; and *Bt* β₁(1-197) containing only the H-NOX domain; 2) two H-NOX mutants, P114A *Cb* and P115A *Cs* H-NOXs.

The authors declare no conflict of interest.

scale rule” hypothesis has so far been validated by all experimental data and it may guide future designs for heme-based gas sensors.

Graphical Abstract



The gaseous ligand selectivity of soluble guanylate cyclase (sGC) obeys the “sliding scale rule”. sGC excludes oxygen binding through the proximal strain of heme and enhanced affinity for NO by multiple-step NO binding.

Keywords

sliding scale rule; soluble guanylate cyclase; gaseous ligand selectivity; heme sensor/binding proteins

1. Introduction

Carbon monoxide (CO), nitric oxide (NO), and oxygen (O₂) are small diatomic gas molecules similar in molecular size and water solubility. They are generated in living organisms by various pathways and often play important messenger roles to trigger various physiological responses [1,2]. To sense these gaseous messengers, living organisms have evolved a variety of machineries, among which heme sensor proteins are widely distributed [3]. Binding of NO, CO, or O₂, referred to as gaseous ligands hereinafter, to prosthetic heme leads to conformational change(s) in heme sensor proteins, initiating downstream response cascades. Although the gaseous ligands differ only by one $2p$ electron from CO to NO to O₂,

the difference in their electronic configuration leads to sharp difference in their affinity for heme [4,5]. On the other hand, concentrations of these molecules fluctuate widely at different locations in living organisms and in their environments; physiological [NO] typically varies from nM to several μM [6], $[\text{O}_2]$ can reach up to hundreds of μM , while [CO] varies between 2.1 to 5.0 nM [7,8,9]. Heme sensor proteins therefore face the challenge to selectively bind one of these molecules in the presence of the other two. There have been extensive studies on the mechanism of gaseous ligand selectivity in a variety of hemoproteins. One important example of heme sensor proteins is the only mammalian NO receptor soluble guanylate cyclase (sGC), exhibiting an extremely high affinity for NO but excludes any binding of O_2 . The remarkable selectivity of sGC among the gaseous ligands enables it to sense less than nM NO under aerobic conditions, where $[\text{O}_2]$ is $\sim 260 \mu\text{M}$. The underlying mechanism of this phenomenal gaseous ligand selectivity of sGC has been investigated for more than 40 years. Only recently a clear picture gradually evolved, based on structural and kinetic data from various heme models and hemoproteins including sGC and its structural analog bacterial Heme NO/Oxygen-binding proteins (H-NOXs). In this short review, we will discuss the factors that determine ligand selectivity of heme sensor proteins with a focus on the gaseous ligand discrimination by sGC and its NO binding.

2. sGC Selectively Binds NO but not O_2

sGC is the only authentic mammalian heme-based sensor and acceptor for NO leading to stimulation of downstream pathway. For example, in human cardiovascular and pulmonary systems, NO synthesized from L-arginine by endothelial nitric oxide synthase in the endothelium of blood vessels diffuses to platelets or adjacent vascular smooth muscle cells (VSMCs) and interacts with cytosolic sGC, leading to several hundred fold activation of its guanosine 3',5'-cyclic monophosphate (cGMP) synthesis activity. The increased level of cGMP stimulates cGMP effectors including cGMP-specific protein kinase, phosphodiesterases, and cyclic nucleotide gated channels; leading to a variety of cellular and physiological events. The effects of sGC activation include calcium sequestration and cytoskeletal changes, relaxation of VSMCs and improved oxygenation of tissues and organs [10], facilitation of the repair of injured endothelium [11,12], inhibition of adhesion and subsequent migration of leukocytes [13], reduction of platelet aggregation [14,15], and inhibition of proliferation and migration of VSMCs [16]. It is not surprising that sGC is an important and active therapeutic target. NO-generating nitrovasodilators such as nitroglycerin and isosorbide mononitrate are used to up-regulate sGC function to manage heart failure, angina, and hypertensive crisis [17].

sGC is a heterodimer, consisting of an α and a β subunits, each containing an H-NOX domain, a Per-Arnt-Sim domain (PAS), a coiled-coil domain (CC), and a catalytic domain (CAT). Only the β H-NOX domain contains a heme prosthetic group [18,19,20,21,22]. Cryogenic electron microscopy (cryo-EM) of dimeric sGC shows a two-lope structure with the H-NOX/PAS domains on one end and the CAT domains on the other, connected by the CC domains. The structure reveals that β CC helix has a contact with the β H-NOX domain and the CC domains form a bend in inactive sGC [23,24]. NO binding to the heme triggers a relative rotation among α and β CC helices and unbending in the CC domains while maintaining the β CC helix contact with the β H-NOX domain. Transduction of the CC

rotation to the CAT domains leads to rotation in the latter and formation of a binding pocket with more optimal binding of substrate GTP and the catalysis of cGMP synthesis [23,24]. CO also binds to sGC but its binding only leads to a fourfold stimulation of enzymatic activity over the basal level [18,19]. Intriguingly, there is no O₂ binding to sGC even at concentrations as high as 1.3 mM (solubility of 1 atm O₂ in aqueous solution [25]). This dramatic ligand selectivity enables sGC to sense minimal NO signal in the presence of enormous amount of O₂ [26]. How does sGC exhibit such power in discriminating NO and O₂? Recently proposed “sliding scale rule” provides a clear explanation for this puzzle.

3. The “Sliding Scale Rule” Hypothesis

The “sliding scale rule” hypothesis is derived from the binding data of all three gaseous ligands from hundreds heme model compounds and hemoproteins with varying protein folds to interpret the gaseous ligand selectivity in a plethora of hemoproteins, including sGC [27]. Through the bioinformatic graphical analysis of gaseous ligand affinity data versus gaseous ligand type, it reveals a general pattern in the gaseous ligand binding to hemoproteins [4,27]. Since its proposal, complete kinetics data were obtained for several additional hemoproteins; and all these data corroborate the pattern revealed by the “sliding scale rule” [28,29,30,31]. The “sliding scale rule” hypothesis identifies five key factors that govern the gaseous ligand selectivity of hemoproteins: (i) the identity of the proximal ligand; (ii) the proximal strain of heme; (iii) distal steric hindrance; (iv) hydrogen-bond (H-bond) donor(s) in the distal pocket; and (v) multiple-step NO binding (Fig. 1). The “sliding scale rule” hypothesis emphasizes that a five-coordinated (5c) heme ligated to a neutral histidine possesses intrinsic selectivity for NO, CO, and O₂ while protein-derived structural elements modify this intrinsic selectivity to adapt to different functional requirements (Fig. 1). Since the proposal of the “sliding scale rule”, the governing power of these five factors for gaseous ligand binding in hemoproteins has been further substantiated in several recent studies. In the following sections, each factor is discussed in more details, emphasizing new enlightenment revealed by recent studies. Two recent data which provide new insights into gas ligand selectivity by hemoproteins are also discussed.

3.1. Intrinsic gaseous ligand selectivity of hemoproteins

The significantly different affinities for NO, CO, and O₂ observed in some hemoproteins root in the intrinsic property of the heme ligated to a neutral histidine proximal ligand. Such intrinsic gaseous ligand selectivity is well manifested by heme model compound protoporphyrin IX 1-methylimidazole (PP(1-MeIm)), which shows remarkably large affinity ratios, $K_D(\text{CO})/K_D(\text{NO}) \approx K_D(\text{O}_2)/K_D(\text{CO}) \approx 10^3 - 10^4$ (Fig. 1A). This pronounced difference in the binding affinity of PP(1-MeIm) for NO, CO, and O₂ is determined by the optimal strength of a proximal neutral imidazole ligand. Such significant intrinsic gaseous ligand selectivity is borne out in many hemoproteins with a proximal histidine ligand, such as globins, sGC, and bacterial H-NOXs [27]. Hemoproteins also bear other types of proximal ligands, such as imidazolate in many peroxidases [32], cysteine thiolate in cytochrome P450s [33], or tyrosine phenolate anion in catalase [32]; however, these ligands have more electron donating property and are therefore much stronger ligands, which suppress differential in affinity for NO, CO, and O₂, leading to the so-called “leveling

effect” [27]. For simplicity, hemoproteins in the following text only refer to those with a 5c heme ligated to a neutral histidine. Due to approximately equal affinity ratios between two ligand pairs, $K_D(\text{CO})/K_D(\text{NO}) \approx K_D(\text{O}_2)/K_D(\text{CO})$, the logarithms of the gaseous ligand affinity ($\log K_D(\text{NO})$, $\log K_D(\text{CO})$, and $\log K_D(\text{O}_2)$) in a hemoprotein fall on an approximately straight line when plotted as a function of the ligand type (Fig. 1A). Moreover, such lines in different hemoproteins parallel each other due to the similar values of the ligand affinity ratios. An immediate application based on the linearity of these $\log K_D(\text{NO})$ - $\log K_D(\text{CO})$ - $\log K_D(\text{O}_2)$ lines is that, as long as the affinity of one gaseous ligand is known, it is possible to estimate the affinity of other gaseous ligand(s) which is difficult to measure. For example, $K_D(\text{O}_2)$ for sGC can be estimated to be ~ 1.3 M, by drawing a line through its measured $K_D(\text{NO})$ or $K_D(\text{CO})$ parallel to the data obtained for a heme model (Fig. 1A).

The $10^3 - 10^4$ fold intrinsic selectivity between NO/CO and between CO/O₂ afforded by a neutral histidine-ligated heme may be inadequate for a hemoprotein to selectively bind NO, CO, or O₂ whose levels vary in a range wider than $10^3 - 10^4$ inside living organisms or in their environments. The concentration of O₂ in aqueous solution under atmospheric pressure reaches ~ 260 μM , on the other hand, the basal [NO] inside a living organism is only around pM. Moreover, the level of NO, CO, and O₂ also fluctuates dramatically inside living organisms under different physiological and pathological conditions. To meet such a large dynamic range of gas sensing, hemoproteins have evolved mechanisms to modulate the intrinsic discriminating ability of a neutral histidine-ligated heme for gaseous ligands either in a non-selective way, where the affinity for all three gaseous ligands are uniformly adjusted, or selectively for either O₂ or NO. Two major protein-dependent factors which uniformly shift the intrinsic affinity of hemoproteins for all three gaseous ligands are the proximal strain of heme and steric hindrance on the distal side of heme.

3.2. Proximal strain of heme

Proximal strain adjusts the Fe-His bond strength between heme and its proximal histidine ligand [34,35,36], modulating the bond formation between heme Fe atom and a ligand on the distal side by regulating both on-rate (k_{on}) and off-rate (k_{off}) of a gaseous ligand to and from the heme, respectively (Fig. 1A) [27]. The Fe-His bond strength in a hemoprotein compared to a heme model compound(s) attunes the intrinsic affinity of heme for all three ligands but maintain the affinity ratios. For example, sGC shows two-order lower affinity for all three gases compared to bacterial H-NOXs (Fig. 1A) [30], which is most likely due to the elevated proximal strain in sGC as suggested by several experimental data. First, sGC has a longer Fe-His bond than bacterial H-NOXs [23,37,38,39]. The longer and weaker Fe-His bond in 5c sGC compared to that in model heme or typical b-type hemoproteins like myoglobin is corroborated by infrared spectroscopy (IR) data for sGC, $\nu_{\text{Fe-His}} = 204$ cm^{-1} . Moreover, IR data also shows a weak Fe-CO bond in CO-bound sGC, with $\nu_{\text{Fe-CO}} = 472$ cm^{-1} [40,41]. Second, the midpoint potential (E_M) of sGC from different species, +187 mV for human sGC and +234 mV for sGC from *Manduca sexta* (*Ms* sGC), is very high for a hemoprotein with a histidine proximal ligand, such as myoglobin and other b-type hemoproteins [42,43]. These values are in line with the striking difference of His-Fe bond strength in sGC, as compared to other hemoproteins. As discussed below, it was recently

revealed that the proximal strain in the β_1 H-NOX domain of sGC is partially due to the interactions between its α and β subunits and between the different domains in its β subunit.

The bacterial H-NOXs, whose affinity for the three gaseous ligands have been measured, all have a single domain structure, either the stand-alone protein in a facultative anaerobe, such as the H-NOXs from *Nostoc* sp. PCC7120 (*Ns* H-NOX), *Shewanella oneidensis* (*So* H-NOX), and *Vibrio cholera* (*Vc* H-NOX) [28,30], or the H-NOX domain of a methyl-accepting chemotaxis protein (MCP) in an obligatory anaerobe, such as *Clostridium botulinum* (*Cb* H-NOX) and *Caldanaerobacter subterraneus subsp. tengcongensis* (*Cs* H-NOX)ⁱ [29,44,45,46]. sGC, on the other hand, is a heterodimer (α and β subunits) each containing multiple domains. Recently, the $K_D(\text{CO})$ of sGC β_1 H-NOX was shown to be modulated by the interactions between the α and β subunits and between the domains in its β subunit [47]. Truncated $\beta_1(1-380)$ of *Ms* sGC including H-NOX, PAS, and CC domains, has a $K_D(\text{CO}) = 0.2 \mu\text{M}$, which is slightly lower than those of bacterial H-NOXs but more than 3 orders of magnitude lower than that of full length sGC, $K_D(\text{CO}) = 260 \mu\text{M}$ [47]; its heterodimers with truncated $\alpha_1(49-450)$ and $\alpha_1(272-450)$ have $K_D(\text{CO}) = 50$ and $2.2 \mu\text{M}$, respectively, revealing a reverse correlation with the extent of α_1 truncation [47]. Dimerization with the α_1 subunit therefore decreases the CO-binding affinity of the β_1 H-NOX, suggesting that wild-type sGC is in an “inhibitory” form with low affinity for CO, and removal of the α_1 subunit removes the inhibition and restores the intrinsic high-affinity CO binding of the β_1 H-NOX. Furthermore, other domain(s) of the β_1 subunit also modulates its affinity for CO. This is indicated by the decrease in $K_D(\text{CO})$ value from $127 \mu\text{M}$ to $15 \mu\text{M}$ and to $1.6 \mu\text{M}$ for wild type bovine sGC (*Bt* sGC, $\alpha_1(1-691)/\beta_1(1-619)$), and *Bt* sGC $\beta_1(1-359)$ and $\beta_1(1-197)$ constructs, respectively [47]. To complete the data set of gaseous ligand affinity in *Bt* sGC $\beta_1(1-359)$ and $\beta_1(1-197)$, we examined the affinity of these sGC constructs for NO and O₂ (Figs. S1 and S2 and Table S1, Supplementary Information). Although $K_D(\text{NO})$ of sGC $\beta_1(1-197)$ could not be experimentally determined, *Bt* sGC $\beta_1(1-359)$ shows significantly stronger affinity for NO than full length sGC, but has no affinity for O₂ (Table S1), corroborating the “sliding scale rule”. Although no oxyferrous complex is observed in *Bt* sGC $\beta_1(1-359)$, ferrous *Bt* sGC $\beta_1(1-359)$ slowly autoxidizes in prolong incubation with O₂ (Fig. S3A, inset), in line with stronger affinity for all three gaseous ligands in this construct compared to full length sGC. Overall, these data and the previous study suggest that the interactions between the α_1 and β_1 subunit and between the β_1 domains in sGC weaken its Fe-His bond and lead to weaker gaseous ligand affinity. The mechanism of modulation in Fe-His bond strength by the subunit-subunit and the domain-domain interactions in sGC calls for further investigation. Modulation of gaseous ligand affinity by subunit-subunit interaction is also found in hemoglobin (Hb), which shows significantly stronger affinity for all three gases in its R-state than T-state [35]. It will also be interesting to measure the affinity of *Cb* and *Cs* H-NOX domains in full length MCPs and compare with those of isolated *Cb* and *Cs* H-NOXs [29,44].

Overall, sGC achieves exclusion of O₂ binding by profoundly decreasing its intrinsic affinity for all three gases through significant proximal strain of its heme exerted by its structural

ⁱ*Cs* H-NOX was formerly known as *Tt* H-NOX (H-NOX from *Thermoanaerobacter tengcongensis*).

fold as a whole (Fig. 1A). The exclusion of O₂ binding in sGC is astonishing, as no O₂ binding to sGC is observable even in O₂ saturated buffer. The K_D(O₂)_{sGC} can be predicted by the “sliding scale rule” to be ~ 1.3 M, far higher than [O₂] in solution under 1 atm pure O₂ (Fig. 2A).

Proximal strain of heme could also be fine-tuned by the orientation of the imidazole ring of proximal histidine relative to the tetrapyrroles of heme porphyrin. Two types of conformers due to such orientation are observed, an “eclipsed” conformation where the imidazole ring approximately parallels the line connecting the nitrogen atoms of two opposite heme pyrroles, and a “staggered” conformation where the imidazole ring roughly parallels the line connecting two opposite methine carbons of the heme [4,35]. A “staggered”, or more relaxed conformation, observed in L16A cytochrome *c*' (Cyt *c*') [48,49,50] and H16L leghemoglobin (Lb) [51,52,53], renders the heme much stronger affinity for gaseous ligand than an “eclipsed”, more constrained conformation, as observed in myoglobin (Mb) and its mutants [35,54,55,56]. The recent cryo-EM structure of sGC shows that the imidazole ring of proximal His105 adopts an “eclipsed” conformation [23]. Heme model protoporphyrin IX 1-methylimidazole (PP(1-MeIm)) does not have protein component to hold the orientation of its imidazole ring, leading to significant flexibility in ring rotation and therefore exhibits affinity for gaseous ligands between those of L16A Cyt *c*' and Mb.

3.3. Distal steric hindrance

Some hemoproteins modulate the association with and dissociation from the heme of a gaseous ligand, therefore modifying its k_{on} and k_{off} , by steric hindrance of a bulky amino acid sidechain(s) on the distal side of the heme [50,57]. Just like proximal strain, distal steric hindrance in a hemoprotein indiscriminately lowers the affinity of its heme for all three gaseous ligands. Distal steric hindrance is best exemplified by the profound effect of a single L16A mutation on K_Ds of L16A Cyt *c*'. In L16A Cyt *c*', replacing bulky Leu16 with alanine in the heme distal pocket removes the distal steric hindrance. Such replacement leads to large increase in k_{on} and decrease in k_{off} , resulting in an increase of ~ 8 orders of magnitude in affinity of L16A Cyt *c*' for all three ligands than wt Cyt *c*' (Fig. 1B) [27,57]. On the other hand, the near diffusion-limited k_{on} (NO) in sGC indicates that NO binding is unimpeded in sGC, despite the bulky Phe74 is located near heme iron on the distal side of sGC, likely imposing some “distal steric hindrance” [23].

A factor conceptually similar to “distal steric hindrance” factor is “distal pocket bulkiness” which is proposed to explain the gaseous ligand selectivity in *Cs* H-NOX. Introducing a bulky residue sidechain(s) into *Cs* H-NOX heme distal pocket leads to a decrease in its affinity for O₂, although the effects on NO and CO binding is not determined [58,59]. The effects of such mutations include increased flexibility of heme, weakening of H-bonding to bound O₂, and changing in conformation of the imidazole ring of the proximal histidine ligand [58,59,60], and the structural and kinetic changes depend heavily on which residue is mutated. However, compared to the effect of “distal steric hindrance” factor in gaseous ligand binding established using L16A Cyt *c*', the data for establishing the “distal pocket bulkiness” factor is much less in extent and rather non-specific [50,57].

Through proximal strain and/or distal steric hindrance, hemoproteins dramatically expand their range of affinity for NO, CO, and O₂ by about 8 – 9 orders of magnitude, without altering the intrinsic $K_D(\text{CO})/K_D(\text{NO})$ and $K_D(\text{O}_2)/K_D(\text{CO})$ ratios of a neutral histidine-ligated heme [27]. The modulation power of protein structural elements is demonstrated by the approximately parallel $\log K_D(\text{NO})$ - $\log K_D(\text{CO})$ - $\log K_D(\text{O}_2)$ lines of different hemoproteins, vertically sliding in a dynamic range of ~ 9 orders of magnitude (Fig. 1A and B). The term “sliding scale rule” is derived from the parallel lines of $\log K_D$ (Fig. 1A and B).

Hemoproteins do not always attune the affinity of heme for the three gaseous ligands equally. In many cases, hemoproteins enhance the affinity of heme for only one of the gases, particularly NO or O₂. In these hemoproteins, the $\log K_D(\text{NO})$ - $\log K_D(\text{CO})$ - $\log K_D(\text{O}_2)$ lines bend down on either end, appearing as deviation or outlier to the “sliding scale rule” paradigm (Fig. 1C and D). The non-selective modulation for the affinity of each gaseous ligand and selective modulation for a particular gas are often combined to meet the functional requirement of a hemoprotein. Some hemoproteins that function as sensor or transporter for O₂ boost their affinity for O₂ through a distal H-bond donor(s). On the other hand, the affinity of sGC for NO is selectively enhanced to compensate for the substantially weakened affinity for all three gases through the proximal strain to exclude O₂ binding; this phenomenal selectivity for NO in sGC, also in other H-NOXs, is achieved through multiple-step NO-binding mechanism. Such selectivity is elaborated below.

3.4. Distal hydrogen bond donor

A H-bond donor(s) in a hemoprotein forms H-bond to heme-bound O₂ and stabilizes the oxyferrous complex, leading to a significantly decreased $K_D(\text{O}_2)$ with little or no effect on CO or NO binding (Fig. 1C). In many hemoproteins, distal H-bond donor(s) is often the most effective way to enable them to bind O₂, since O₂ has the lowest intrinsic affinity for heme and an oxyferrous complex is often unstable without additional means of stabilization. Distal histidine in Hb and Mb are good examples with distal H-bond donors that stabilize oxyferrous heme (Fig. 1C) [4]. The major factor in discriminating NO, CO, and O₂ in Mb or Hb is ascribed to this electrostatic H-bond donor [61]. However, existence of a distal H-bond donor(s) is certainly not the only factor to enable O₂ binding in a hemoprotein; L16A Cyt *c*, which shows a strong affinity for O₂, $K_D(\text{O}_2) = 49$ nM, is a perfect illustration of how protein-dependent environments are able to regulate O₂ binding without a H-bond donor in certain hemoproteins [50].

In bacterial H-NOXs, it is noticed that several bacterial H-NOXs from obligatory anaerobic bacteria, such as *Cb* and *Cs* H-NOXs, have a tyrosine, Tyr139 and Tyr140, respectively, in the distal pocket; both *Cb* and *Cs* H-NOXs exhibit strong affinity for O₂ [29]. The crystal structure of *Cs* H-NOX shows that Tyr140 forms an H-bond to its oxyferrous complex [39]. On the other hand, H-NOXs from facultative bacteria, such as *Vc* and *So* H-NOXs do not have distal H-bond donor and exhibit no measurable affinity for O₂. Moreover, removing H-bond donor in *Cb* and *Cs* H-NOXs leads to no measurable affinity for O₂ in Y139F *Cb* H-NOX and Y140F *Cs* H-NOX [29,46]. A distal H-bond donor is therefore sufficient to render O₂ binding in bacterial H-NOXs. Based on the observations of H-NOXs, it is deduced that the lack of a distal pocket H-bond donor in sGC eliminates O₂ as a ligand, leading to its

selectivity for NO [62,63]. However, experimental data show that introduction of a H-bond donating tyrosine residue in the vicinity of the distal side of sGC heme (I145Y sGC) does not lead to O₂ binding [64], highlighting some crucial difference between sGC and its bacterial H-NOX analogs. Due to the lack of the 3D structure of I145Y sGC, it is hard to confirm that the side chain of introduced Tyr145 is oriented optimally for H-bonding to O₂ ligand, nevertheless, the study suggests that distal H-bond donor(s) may not be an efficient factor to introduce O₂ binding in some hemoproteins.

3.5. Multiple-step NO binding

Multiple-step NO binding dramatically enhances the apparent affinity for NO in a hemoprotein and is best demonstrated by the NO binding in sGC. In the presence of stoichiometric or substoichiometric amount of NO, sGC binds NO reversibly to form a 6-coordinate (6c) NO-heme complex at $k_{\text{on}} = 1.4 \times 10^8 \text{ M}^{-1}\text{s}^{-1}$ and $k_{\text{off}, 6\text{c}} = 27 \text{ s}^{-1}$, yielding an intrinsic $K_{\text{D}}(\text{NO}) = k_{\text{off}, 6\text{c}}(\text{NO})/k_{\text{on}}(\text{NO}) = 54 \text{ nM}$ (Fig. 3, A \leftrightarrow B) [27,45]. This $K_{\text{D}}(\text{NO})$ indicates that NO binding is not very strong in sGC with the initial formation of the 6c NO-heme complex. Once formed, the Fe-His bond in the 6c NO-heme complex breaks at a rate of 8.5 s^{-1} , irreversibly converting to a 5-coordinate (5c) NO-heme complex with NO on the distal side (5c NO_d) (Fig. 3, B \rightarrow E). On the other hand, in the presence of excess NO, the initially formed 6c NO-heme complex in sGC reacts with another NO at $k_{\text{on}} = \sim 10^6 \text{ M}^{-1}\text{s}^{-1}$ and $k_{\text{off}} = 26 \text{ s}^{-1}$, forming a transient quaternary complex which irreversibly converts to another 5c NO complex at $> 600 \text{ s}^{-1}$, with NO sitting on the proximal side (5c NO_p) (Fig. 3, B \leftrightarrow C \rightarrow D) [65]. Either 5c NO_d or 5c NO_p has a significantly lower dissociation rate constant than 6c NO-heme, $k_{\text{off}, 5\text{c}}(\text{NO}) \sim 1.1 \times 10^{-3} \text{ M}^{-1} \ll k_{\text{off}, 6\text{c}}(\text{NO})$, therefore conversion of 6c to either 5c complex results in $K_{\text{D}}(\text{NO})_{\text{apparent}} = k_{\text{off}, 5\text{c}}(\text{NO})/k_{\text{on}}(\text{NO}) = 7.1 \text{ pM}$ (Fig. 2D), dramatically enhancing the apparent affinity of sGC for NO [27]. Such NO affinity enhancement through multiple-step NO binding is also seen in many other hemoproteins, such as bacterial *Vc* and *So* H-NOXs. Similar to sGC, formation of the 5c NO complex in bacterial H-NOXs leads to much decreased $K_{\text{D}}(\text{NO})_{\text{apparent}} = 1 - 7.3 \text{ pM}$ [28,29,30]. The conversion of a 6c NO-heme complex to a 5c NO-heme complex is due to the strong negative *trans* effect of NO which weakens Fe-His bond opposite of NO, therefore, multiple-step NO binding is a mechanism which leads to enhancement in NO affinity only [49].

There has been controversy whether 5c NO_p is formed in sGC in the presence of excess NO since distal- and proximal-specific 5c NO-heme complexes, or 5c NO_d and 5c NO_p, are indistinguishable via optical spectroscopy or electron paramagnetic resonance (EPR) method. The 5c NO_p complex is found in the crystal structures of Cyt *c'* from *Alcaligenes xylosoxidans* [49] and *So* H-NOX [66]. One study addresses the sidedness of 5c NO-heme in sGC using sequential stopped-flow to follow the spectral change in sGC reacting with stoichiometric or excess NO, and parallel two-stage rapid-freeze quench EPR to exam the hyperfine EPR structure of the trapped 5c NO-heme complex, reacting sGC first with ¹⁴NO and then ¹⁵NO, or vice versa [65]. EPR data of the final 5c NO-heme complex trapped using varying levels of ¹⁴NO and ¹⁵NO indicate that the 2nd NO binds to the proximal side of the heme. This data suggests that either 5c NO_d or 5c NO_p, formed in sGC in the presence of

stoichiometric and excess NO, respectively, activates sGC similarly, in line with the study showing that either 5c NO_d or 5c NO_p leads to similar spiking cGMP formation [67].

Another study follows the time-resolved absorption change in NO rebinding to heme after photolysis of 5c NO-heme complex in sGC [68]. Other than germinate NO rebinding to heme with a $\tau = 6.5$ ns, 2nd order rebinding of NO to sGC (20 μ M) proceeds with $\tau = 250$ μ s (1 \times NO) and 50 μ s (10 \times NO); and the formed 6c NO-heme converts to 5c NO-heme with $\tau = 43$ ms and 10 ms, respectively [68]. Due to lack of the detection of dinitrosyl heme (Fig. 3, C), it is concluded that NO only binds heme from distal side within millisecond time scale. However, transient formation of dinitrosyl heme is not excluded [68]. In another study in much longer time scale, the sidedness of 5c NO-heme complex in *So* H-NOX is inferred from the distance between NO and a spin label attached to *So* H-NOX measured by double electron-electron resonance (DEER) [69]. It is found that 5c NO_d is prominent at both < 1 \times and excess NO treatments of *So* H-NOX. For this to happen, it is assumed that the 6c NO-heme to 5c NO-heme conversion in the presence of excess NO is highly reversible (Fig. 3, C \leftrightarrow D) [69]. However, this assumption is at odds with the kinetic measurements showing that *So* H-NOX reacts with excess NO to generate 5c NO_p irreversibly at a rate > 600 s⁻¹ [27,30,45]. The conclusion by DEER study also contradicts the structural data which show 5c NO_p in the crystal structure of *So* H-NOX reacted with excess NO [66].

When reacting with excess NO, certain cysteine residue(s) in sGC are proposed to form *S*-nitrosylthiol radical anion ($-\text{RSNO}^{\cdot-}$), albeit empirical explanation seems supporting the existence of such radical anion, direct evidence such as EPR characterization, remains to be provided [70]. It is also hard to rationalize the observed heme spectral change caused by a cysteine nitrosylation. Such secondary cysteine modification has been proposed to be necessary for full activation of sGC and the initial NO binding to heme is shown to only partially activate sGC [70,71,72,73]. On the other hand, a variety of sGC stimulators and activators, such as YC-1 [74,75,76], BAY 41-2272 [77], BAY 58-2667 [78], HMR-1766 [79], and BAY 60-2770 [80], stimulate sGC either by sensitizing sGC to CO and NO or through a heme-independent mechanism. However, these sGC activation mechanisms are unlikely linked directly to selective NO binding in sGC.

4. Other Factors Proposed to Affect Gaseous Ligand Binding

In addition to the factors determined in the “sliding scale rule” hypothesis, several other factors have been proposed to address the selectivity of gaseous ligands in sGC and bacterial H-NOXs.

4.1. Hydrophobic heme pocket

It is noticed that the distal heme pocket in sGC is quite hydrophobic [23], potentially favoring binding of a gaseous ligand [81,82]. However, due to the similar physical properties of the three gaseous ligands, hydrophobicity of heme pocket unlikely shows significant discrimination among the three gases. So far there is no detailed kinetic study to evaluate any effect of the hydrophobicity of distal pocket on selective binding of gaseous ligands in hemoproteins.

4.2. Ligand access path

Efforts have been made to probe the access path(s) for gaseous ligands onto the distal side of heme and a Y-shaped gas access channel is identified by equilibrium xenon (Xe) binding site(s) in *Ns* H-NOX [66,83]. Moreover, kinetics of CO binding is found to be modified in the H-NOX mutants using bulky tryptophan to replace key residues lining the tentative channel(s) [66,83]. The identification of such channels raised several concerns: (i) CO is not an appropriate ligand to assess kinetic binding for its intrinsically much smaller k_{on} to ferrous heme than those of NO or O₂, due to spin limitation [84]; (ii) it is demonstrated that thermodynamic Xe binding to hemeprotein does not necessarily represent the kinetic ligand access to the iron [85]; (iii) the near diffusion-limited k_{on} of both NO and O₂ binding in sGC and several H-NOXs [27,30] indicate little restriction in ligand access; and (iv) it is revealed in several crystal structures of H-NOXs [37,38,39]; a much shorter ligand path from the solvent leading directly to the side of the heme and is proposed to be a more efficient alternative path [30]. Both Y-shaped gas access channel and the short access path are noted in a recent molecular dynamics (MD) calculation on *Ns* and *So* H-NOXs. The MD calculations also identifies a third channel and *Ns* and *So* H-NOXs show different preference for these channels [86]. Overall, the near diffusion limit $k_{\text{on}}(\text{NO})$ rate constants in bacterial H-NOXs and sGC suggest that gas access channel(s) in these hemoproteins does not play any significant role in their gaseous ligand selectivity.

4.3. Heme distortion

Structural data of several bacterial H-NOXs show that the heme is significantly distorted from planar geometry and such heme deformation is proposed to modulate gaseous ligand affinity [38,87]. In sGC and all known bacterial H-NOXs, a conserved proline is located on the heme proximal side (Pro118 in sGC) [39]. The orthologous proline in *Cs* H-NOX (Pro115) or *So* H-NOX (Pro116) buttresses the heme porphyrin plane and promotes heme distortion in both H-NOXs [39,66]. Heme distortion caused by proline buttress is proposed to play a role in the gaseous ligand selectivity of the bacterial H-NOXs based on several lines of experimental observations. First, P115A *Cs* H-NOX has a flattened heme, a large +167 mV to -4 mV shift in E_{M} , and a 217 to 223 cm⁻¹ shift in resonance Raman (rR) $\nu_{\text{Fe-His}}$ band, implying strengthening of the Fe-His bond [88]. However, rR data also indicated that Fe-CO bond strength remains unchanged and the Fe-O₂ bond strength is even weakened [89]. P115A *Cs* H-NOX shows a slightly increased affinity for O₂ compared to wild type *Cs* H-NOX, a 4.5 \times decrease in $K_{\text{D}}(\text{O}_2)$, due to somewhat increased $k_{\text{on}}(\text{O}_2)$ and slightly decreased $k_{\text{off}}(\text{O}_2)$ [87]. Second, in bacterial H-NOX from *Shewanella woodyi* (*Sw* H-NOX), mutating the corresponding Pro117 to alanine results in a relaxed planar heme and a 10-fold increase in the coupled phosphodiesterase activity, similar to that by NO-activated *Sw* H-NOX [38].

The E_{M} shift and increase in Fe-His bond strength in P115A *Cs* H-NOX compared with the wild-type suggest that the heme distortion leads to enhanced proximal strain in *Cs* H-NOX [87]. However, the enhancement in O₂ affinity for P115A *Cs* H-NOX compared to wild type *Cs* H-NOX is rather small. Furthermore, the small $K_{\text{D}}(\text{O}_2)$ of *Cs* H-NOX is mostly due to its distal H-bond donor, Tyr140, which does not play any significant role in the binding of NO and CO [29]. It is difficult to assess the proximal strain introduced by Pro115 only based on

kinetic data of O₂ binding. We therefore measured the kinetic and affinity of P114A *Cb* and P115A *Cs* H-NOXs for each gaseous ligand (Figs. S5 - S7 and Table S1, Supplementary Information). The gaseous ligand binding in P114A *Cb* and P115A *Cs* H-NOXs follows the “sliding scale rule” and the $K_D(\text{NO})$, $K_D(\text{CO})$, and $K_D(\text{O}_2)$ of P114A *Cb* and P115A *Cs* H-NOXs show no significant change compared with those of wt *Cb* and *Cs* H-NOXs, respectively. On the other hand, these data suggest that the heme distortion introduced by the buttressing proline residue unlikely alters the proximal strain of heme in either *Cb* or *Cs* H-NOX and is not a major factor dictating the affinity and selectivity for gaseous ligands in these H-NOXs. The relationship between heme distortion and the proximal strain of heme warrants further investigation.

5. Summary and Perspective

The “sliding scale rule” hypothesis identifies five major factors determining the gaseous ligand selectivity of hemoproteins. This hypothesis elucidates the gaseous ligand selectivity by sGC as a result of: 1) the prosthetic heme ligated to a neutral His105 provides sGC intrinsic selectivity among NO, CO, and O₂, 2) proximal strain of sGC heme governed by the subunit-subunit and the domain-domain interactions greatly decreases its affinity for all three gaseous ligands and achieve complete exclusion of O₂; 3) multiple-step NO binding greatly enhances sGC effective affinity for NO.

The mechanism revealed by the “sliding scale rule” for sGC’s phenomenal NO selectivity may also have implications on a unified model on NO-activation, deactivation, and re-activation of sGC (Fig. 4). In the resting sGC with 5c unliganded ferrous heme, the strong proximal strain of heme renders sGC selectivity for NO. The dissociation of His105 and subsequent domain rearrangement upon NO binding to sGC release proximal strain of heme, leading to higher affinity for all three gaseous ligands (Fig. 4). Soluble guanylate cyclase may thus be deactivated through the NO-dioxygenation of the 5c NO-heme complex and the resulting ferric heme would facilitate re-ligation of His105 to regenerate oxidized 5c-sGC (Fig. 4). Oxidized sGC can be easily re-activated through reduction by either intrinsic or other cellular reductant to its ferrous resting state as a result of the high $E_M(\text{Fe}^{+3}/\text{Fe}^{+2})$, ready for another round of NO-activation (Fig. 4). This model of activation, deactivation, and re-activation of sGC is solely based on NO and O₂ interaction with heme and it will be tested in our future studies.

The “sliding scale rule” hypothesis is so far the most promising one to rationalize all data regarding the selective gaseous ligand binding and sensing of a multitude of hemoproteins; it provides a unified model for gaseous ligand selectivity in hemoproteins and thus deserves more extensive testing in the future to establish a new paradigm for gaseous ligand selectivity.

Supplementary Material

Refer to Web version on PubMed Central for supplementary material.

Acknowledgments

Fund Information. This study is supported by E.G. R21EY026663 (EDG); E.M. R01 HL139838; A.-L. T. R01 DH122784.

References

- [1]. Girvan HM, Munro AW, Heme sensor proteins, *J Biol Chem* 288 (2013) 13194–13203. [PubMed: 23539616]
- [2]. Liebl U, Lambry JC, Vos MH, Primary processes in heme-based sensor proteins, *Biochim Biophys Acta* 1834 (2013) 1684–1692. [PubMed: 23485911]
- [3]. Shimizu T, Huang D, Yan F, Stranova M, Bartosova M, Fojtikova V, Martinkova M, Gaseous O₂, NO, and CO in signal transduction: structure and function relationships of heme-based gas sensors and heme-redox sensors, *Chem Rev* 115 (2015) 6491–6533. [PubMed: 26021768]
- [4]. Tsai AL, Martin E, Berka V, Olson JS, How do heme-protein sensors exclude oxygen? Lessons learned from cytochrome c', *Nostoc punctiforme* heme nitric oxide/oxygen-binding domain, and soluble guanylyl cyclase, *Antioxid Redox Signal* 17 (2012) 1246–1263. [PubMed: 22356101]
- [5]. Spiro TG, Jarzecki AA, Heme-based sensors: theoretical modeling of heme-ligand-protein interactions, *Curr Opin Chem Biol* 5 (2001) 715–723. [PubMed: 11738184]
- [6]. Lundberg JO, Weitzberg E, Gladwin MT, The nitrate-nitrite-nitric oxide pathway in physiology and therapeutics, *Nat Rev Drug Discov* 7 (2008) 156–167. [PubMed: 18167491]
- [7]. Air Quality Guidelines/Carbon monoxide, WHO Regional Office for Europe, Copenhagen, Denmark, 2000.
- [8]. Coburn RF, Blakemore WS, Forster RE, Endogenous carbon monoxide production in man, *J Clin Invest* 42 (1963) 1172–1178. [PubMed: 14021853]
- [9]. Coburn RF, Danielson GK, Blakemore WS, Forster RE 2nd, Carbon Monoxide in Blood: Analytical Method and Sources of Error, *J Appl Physiol* 19 (1964) 510–515. [PubMed: 14174590]
- [10]. Stasch JP, Becker EM, Alonso-Alija C, Apeler H, Dembowski K, Feurer A, Gerzer R, Minuth T, Perzborn E, Pleiss U, Schroder H, Schroeder W, Stahl E, Steinke W, Straub A, Schramm M, NO-independent regulatory site on soluble guanylate cyclase, *Nature* 410 (2001) 212–215. [PubMed: 11242081]
- [11]. Noiri E, Hu Y, Bahou WF, Keese CR, Giaever I, Goligorsky MS, Permissive role of nitric oxide in endothelin-induced migration of endothelial cells, *J Biol Chem* 272 (1997) 1747–1752. [PubMed: 8999856]
- [12]. Noiri E, Lee E, Testa J, Quigley J, Colflesh D, Keese CR, Giaever I, Goligorsky MS, Podokinesis in endothelial cell migration: role of nitric oxide, *Am J Physiol* 274 (1998) C236–244. [PubMed: 9458733]
- [13]. Kubes P, Suzuki M, Granger DN, Nitric oxide: an endogenous modulator of leukocyte adhesion, *Proc Natl Acad Sci U S A* 88 (1991) 4651–4655. [PubMed: 1675786]
- [14]. Radomski MW, Palmer RM, Moncada S, Endogenous nitric oxide inhibits human platelet adhesion to vascular endothelium, *Lancet* 2 (1987) 1057–1058. [PubMed: 2889967]
- [15]. Makhoul S, Walter E, Pagel O, Walter U, Sickmann A, Gambaryan S, Smolenski A, Zahedi RP, Jurk K, Effects of the NO/soluble guanylate cyclase/cGMP system on the functions of human platelets, *Nitric Oxide* 76 (2018) 71–80. [PubMed: 29550521]
- [16]. Seki J, Nishio M, Kato Y, Motoyama Y, Yoshida K, FK409, a new nitric-oxide donor, suppresses smooth muscle proliferation in the rat model of balloon angioplasty, *Atherosclerosis* 117 (1995) 97–106. [PubMed: 8546759]
- [17]. Boerrigter G, Lapp H, Burnett JC, Modulation of cGMP in heart failure: a new therapeutic paradigm, *Handb Exp Pharmacol* (2009) 485–506. [PubMed: 19089342]
- [18]. Childers KC, Garcin ED, Structure/function of the soluble guanylyl cyclase catalytic domain, *Nitric Oxide* 77 (2018) 53–64. [PubMed: 29702251]
- [19]. Derbyshire ER, Marletta MA, Structure and regulation of soluble guanylate cyclase, *Annu Rev Biochem* 81 (2012) 533–559. [PubMed: 22404633]

- [20]. Xiao S, Li Q, Hu L, Yu Z, Yang J, Chang Q, Chen Z, Hu G, Soluble Guanylate Cyclase Stimulators and Activators: Where are We and Where to Go?, *Mini Rev Med Chem* 19 (2019) 1544–1557. [PubMed: 31362687]
- [21]. Makrynitsa GI, Zompra AA, Argyriou AI, Spyroulias GA, Topouzis S, Therapeutic Targeting of the Soluble Guanylate Cyclase, *Curr Med Chem* 26 (2019) 2730–2747. [PubMed: 30621555]
- [22]. Khalid RR, Maryam A, Fadouloglou VE, Siddiqi AR, Zhang Y, Cryo-EM density map fitting driven in-silico structure of human soluble guanylate cyclase (hsGC) reveals functional aspects of inter-domain cross talk upon NO binding, *J Mol Graph Model* 90 (2019) 109–119. [PubMed: 31055154]
- [23]. Kang Y, Liu R, Wu JX, Chen L, Structural insights into the mechanism of human soluble guanylate cyclase, *Nature* 574 (2019) 206–210. [PubMed: 31514202]
- [24]. Horst BG, Yokom AL, Rosenberg DJ, Morris KL, Hammel M, Hurley JH, Marletta MA, Allosteric activation of the nitric oxide receptor soluble guanylate cyclase mapped by cryo-electron microscopy, *Elife* 8 (2019).
- [25]. Truesdale GA, Downing AL, Solubility of Oxygen in Water, *Nature* 173 (1954) 1236.
- [26]. Hall CN, Garthwaite J, What is the real physiological NO concentration in vivo?, *Nitric Oxide* 21 (2009) 92–103. [PubMed: 19602444]
- [27]. Tsai AL, Berka V, Martin E, Olson JS, A "sliding scale rule" for selectivity among NO, CO, and O₂ by heme protein sensors, *Biochemistry* 51 (2012) 172–186. [PubMed: 22111978]
- [28]. Wu G, Liu W, Berka V, Tsai AL, The selectivity of *Vibrio cholerae* H-NOX for gaseous ligands follows the "sliding scale rule" hypothesis. Ligand interactions with both ferrous and ferric Vc H-NOX, *Biochemistry* 52 (2013) 9432–9446. [PubMed: 24351060]
- [29]. Wu G, Liu W, Berka V, Tsai AL, H-NOX from *Clostridium botulinum*, like H-NOX from *Thermoanaerobacter tengcongensis*, Binds Oxygen but with a Less Stable Oxyferrous Heme Intermediate, *Biochemistry* 54 (2015) 7098–7109. [PubMed: 26574914]
- [30]. Wu G, Liu W, Berka V, Tsai AL, Gaseous ligand selectivity of the H-NOX sensor protein from *Shewanella oneidensis* and comparison to those of other bacterial H-NOXs and soluble guanylyl cyclase, *Biochimie* 140 (2017) 82–92. [PubMed: 28655588]
- [31]. Wu G, Zhao J, Franzen S, Tsai AL, Bindings of NO, CO, and O₂ to multifunctional globin type dehaloperoxidase follow the 'sliding scale rule', *Biochem J* 474 (2017) 3485–3498. [PubMed: 28899945]
- [32]. Dunford HB, *Heme Peroxidases* Wiley-VCH, Canada, 1999.
- [33]. Ortiz de Montellano PR, (Ed.), *Cytochrome P450: Structure, Mechanism, and Biochemistry*, Kluwer Academic/Plenum Publishers, New York, 2005.
- [34]. Jain R, Chan MK, Mechanisms of ligand discrimination by heme proteins, *J Biol Inorg Chem* 8 (2003) 1–11. [PubMed: 12459893]
- [35]. Olson JS, Phillips GN, Myoglobin discriminates between O₂, NO, and CO by electrostatic interactions with the bound ligand, *J. Biol. Inorg. Chem* 2 (1997) 544–552.
- [36]. Oertling WA, Kean RT, Wever R and Babcock GT, Factors Affecting the Iron-Oxygen Vibrations of Ferrous Oxy and Ferryl Oxo Heme Proteins and Model Compounds, *Inorg. Chem* 29 (1990) 2633–2645.
- [37]. Ma X, Sayed N, Beuve A, van den Akker F, NO and CO differentially activate soluble guanylyl cyclase via a heme pivot-bend mechanism, *Embo J* 26 (2007) 578–588. [PubMed: 17215864]
- [38]. Erbil WK, Price MS, Wemmer DE, Marletta MA, A structural basis for H-NOX signaling in *Shewanella oneidensis* by trapping a histidine kinase inhibitory conformation, *Proc Natl Acad Sci U S A* 106 (2009) 19753–19760. [PubMed: 19918063]
- [39]. Pellicena P, Karow DS, Boon EM, Marletta MA, Kuriyan J, Crystal structure of an oxygen-binding heme domain related to soluble guanylate cyclases, *Proc Natl Acad Sci U S A* 101 (2004) 12854–12859. [PubMed: 15326296]
- [40]. Deinum G, Stone JR, Babcock GT, Marletta MA, Binding of nitric oxide and carbon monoxide to soluble guanylate cyclase as observed with Resonance raman spectroscopy, *Biochemistry* 35 (1996) 1540–1547. [PubMed: 8634285]
- [41]. Schelvis JP, Zhao Y, Marletta MA, Babcock GT, Resonance raman characterization of the heme domain of soluble guanylate cyclase, *Biochemistry* 37 (1998) 16289–16297. [PubMed: 9819221]

- [42]. Makino R, Park SY, Obayashi E, Iizuka T, Hori H, Shiro Y, Oxygen binding and redox properties of the heme in soluble guanylate cyclase: implications for the mechanism of ligand discrimination, *J Biol Chem* 286 (2011) 15678–15687. [PubMed: 21385878]
- [43]. Fritz BG, Hu X, Brailey JL, Berry RE, Walker FA, Montfort WR, Oxidation and loss of heme in soluble guanylyl cyclase from *Manduca sexta*, *Biochemistry* 50 (2011) 5813–5815. [PubMed: 21639146]
- [44]. Boon EM, Marletta MA, Ligand specificity of H-NOX domains: from sGC to bacterial NO sensors, *J Inorg Biochem* 99 (2005) 892–902. [PubMed: 15811506]
- [45]. Zhao Y, Brandish PE, Ballou DP, Marletta MA, A molecular basis for nitric oxide sensing by soluble guanylate cyclase, *Proc Natl Acad Sci U S A* 96 (1999) 14753–14758. [PubMed: 10611285]
- [46]. Boon EM, Marletta MA, Sensitive and selective detection of nitric oxide using an H-NOX domain, *J Am Chem Soc* 128 (2006) 10022–10023. [PubMed: 16881625]
- [47]. Purohit R, Fritz BG, The J, Issaian A, Weichsel A, David CL, Campbell E, Hausrath AC, Rassouli-Taylor L, Garcin ED, Gage MJ, Montfort WR, YC-1 binding to the beta subunit of soluble guanylyl cyclase overcomes allosteric inhibition by the alpha subunit, *Biochemistry* 53 (2014) 101–114. [PubMed: 24328155]
- [48]. Andrew CR, Green EL, Lawson DM, Eady RR, Resonance Raman studies of cytochrome c' support the binding of NO and CO to opposite sides of the heme: implications for ligand discrimination in heme-based sensors, *Biochemistry* 40 (2001) 4115–4122. [PubMed: 11300792]
- [49]. Hough MA, Antonyuk SV, Barbieri S, Rustage N, McKay AL, Servid AE, Eady RR, Andrew CR, Hasnain SS, Distal-to-proximal NO conversion in hemoproteins: the role of the proximal pocket, *J Mol Biol* 405 (2011) 395–409. [PubMed: 21073879]
- [50]. Garton EM, Pixton DA, Petersen CA, Eady RR, Hasnain SS, Andrew CR, A Distal Pocket Leu Residue Inhibits the Binding of O(2) and NO at the Distal Heme Site of Cytochrome c', *J Am Chem Soc* (2012).
- [51]. Kundu S, Hargrove MS, Distal heme pocket regulation of ligand binding and stability in soybean leghemoglobin, *Proteins* 50 (2003) 239–248. [PubMed: 12486718]
- [52]. Kundu S, Snyder B, Das K, Chowdhury P, Park J, Petrich JW, Hargrove MS, The leghemoglobin proximal heme pocket directs oxygen dissociation and stabilizes bound heme, *Proteins* 46 (2002) 268–277. [PubMed: 11835502]
- [53]. Hargrove MS, Barry JK, Brucker EA, Berry MB, Phillips GN Jr., Olson JS, Arredondo-Peter R, Dean JM, Klucas RV, Sarath G, Characterization of recombinant soybean leghemoglobin and apolar distal histidine mutants, *J Mol Biol* 266 (1997) 1032–1042. [PubMed: 9086279]
- [54]. Quillin ML, Li T, Olson JS, Phillips GN Jr., Dou Y, Ikeda-Saito M, Regan R, Carlson M, Gibson QH, Li H, et al., Structural and functional effects of apolar mutations of the distal valine in myoglobin, *J Mol Biol* 245 (1995) 416–436. [PubMed: 7837273]
- [55]. Draghi F, Miele AE, Travaglini-Allocatelli C, Vallone B, Brunori M, Gibson QH, Olson JS, Controlling ligand binding in myoglobin by mutagenesis, *J Biol Chem* 277 (2002) 7509–7519. [PubMed: 11744723]
- [56]. Carver TE, Brantley RE Jr., Singleton EW, Arduini RM, Quillin ML, Phillips GN Jr., Olson JS, A novel site-directed mutant of myoglobin with an unusually high O₂ affinity and low autooxidation rate, *J Biol Chem* 267 (1992) 14443–14450. [PubMed: 1629229]
- [57]. Antonyuk SV, Rustage N, Petersen CA, Arnst JL, Heyes DJ, Sharma R, Berry NG, Scrutton NS, Eady RR, Andrew CR, Hasnain SS, Carbon monoxide poisoning is prevented by the energy costs of conformational changes in gas-binding haemproteins, *Proc Natl Acad Sci U S A* 108 (2011) 15780–15785. [PubMed: 21900609]
- [58]. Weinert EE, Phillips-Piro CM, Tran R, Mathies RA, Marletta MA, Controlling Conformational Flexibility of an O(2)-Binding H-NOX Domain, *Biochemistry* (2011).
- [59]. Weinert EE, Plate L, Whited CA, Olea C Jr., Marletta MA, Determinants of ligand affinity and heme reactivity in H-NOX domains, *Angew Chem Int Ed Engl* 49 (2010) 720–723. [PubMed: 20017169]
- [60]. Plate L, Marletta MA, Nitric oxide-sensing H-NOX proteins govern bacterial communal behavior, *Trends Biochem Sci* 38 (2013) 566–575. [PubMed: 24113192]

- [61]. Springer BA, Sligar SG, Olson JS, Phillips GN Jr., Mechanisms of Ligand Recognition in Myoglobin, *Chem. Rev* 94 (1994) 699–714.
- [62]. Boon EM, Huang SH, Marletta MA, A molecular basis for NO selectivity in soluble guanylate cyclase, *Nat Chem Biol* 1 (2005) 53–59. [PubMed: 16407994]
- [63]. Boon EM, Marletta MA, Ligand discrimination in soluble guanylate cyclase and the H-NOX family of heme sensor proteins, *Curr Opin Chem Biol* 9 (2005) 441–446. [PubMed: 16125437]
- [64]. Martin E, Berka V, Bogatenkova E, Murad F, Tsai AL, Ligand selectivity of soluble guanylyl cyclase: effect of the hydrogen-bonding tyrosine in the distal heme pocket on binding of oxygen, nitric oxide, and carbon monoxide, *J Biol Chem* 281 (2006) 27836–27845. [PubMed: 16864588]
- [65]. Martin E, Berka V, Sharina I, Tsai AL, Mechanism of binding of NO to soluble guanylyl cyclase: implication for the second NO binding to the heme proximal site, *Biochemistry* 51 (2012) 2737–2746. [PubMed: 22401134]
- [66]. Herzik MA Jr., Jonnalagadda R, Kuriyan J, Marletta MA, Structural insights into the role of iron-histidine bond cleavage in nitric oxide-induced activation of H-NOX gas sensor proteins, *Proc Natl Acad Sci U S A* 111 (2014) E4156–4164. [PubMed: 25253889]
- [67]. Tsai AL, Berka V, Sharina I, Martin E, Dynamic ligand exchange in soluble guanylyl cyclase (sGC): implications for sGC regulation and desensitization, *J Biol Chem* 286 (2011) 43182–43192. [PubMed: 22009742]
- [68]. Yoo BK, Lamarre I, Martin JL, Rappaport F, Negre M, Motion of proximal histidine and structural allosteric transition in soluble guanylate cyclase, *Proc Natl Acad Sci U S A* 112 (2015) E1697–1704. [PubMed: 25831539]
- [69]. Guo Y, Suess DLM, Herzik MA Jr., Iavarone AT, Britt RD, Marletta MA, Regulation of nitric oxide signaling by formation of a distal receptor-ligand complex, *Nat Chem Biol* 13 (2017) 1216–1221. [PubMed: 28967923]
- [70]. Fernhoff NB, Derbyshire ER, Marletta MA, A nitric oxide/cysteine interaction mediates the activation of soluble guanylate cyclase, *Proc Natl Acad Sci U S A* 106 (2009) 21602–21607. [PubMed: 20007374]
- [71]. Russwurm M, Koesling D, NO activation of guanylyl cyclase, *Embo J* 23 (2004) 4443–4450. [PubMed: 15510222]
- [72]. Derbyshire ER, Marletta MA, Butyl isocyanide as a probe of the activation mechanism of soluble guanylate cyclase. Investigating the role of non-heme nitric oxide, *J Biol Chem* 282 (2007) 35741–35748. [PubMed: 17916555]
- [73]. Horst BG, Marletta MA, Physiological activation and deactivation of soluble guanylate cyclase, *Nitric Oxide* 77 (2018) 65–74. [PubMed: 29704567]
- [74]. Friebe A, Koesling D, Mechanism of YC-1-induced activation of soluble guanylyl cyclase, *Mol Pharmacol* 53 (1998) 123–127. [PubMed: 9443939]
- [75]. Friebe A, Mullershausen F, Smolenski A, Walter U, Schultz G, Koesling D, YC-1 potentiates nitric oxide- and carbon monoxide-induced cyclic GMP effects in human platelets, *Mol Pharmacol* 54 (1998) 962–967. [PubMed: 9855623]
- [76]. Friebe A, Schultz G, Koesling D, Sensitizing soluble guanylyl cyclase to become a highly CO-sensitive enzyme, *Embo J* 15 (1996) 6863–6868. [PubMed: 9003762]
- [77]. Becker EM, Alonso-Alija C, Apeler H, Gerzer R, Minuth T, Pleiss U, Schmidt P, Schramm M, Schroeder H, Schroeder W, Steinke W, Straub A, Stasch JP, NO-independent regulatory site of direct sGC stimulators like YC-1 and BAY 41-2272, *BMC Pharmacol* 1 (2001) 13. [PubMed: 11801189]
- [78]. Chester M, Tourneux P, Seedorf G, Grover TR, Gien J, Abman SH, Cinaciguat, a soluble guanylate cyclase activator, causes potent and sustained pulmonary vasodilation in the ovine fetus, *Am J Physiol Lung Cell Mol Physiol* 297 (2009) L318–325. [PubMed: 19465519]
- [79]. Zhou Z, Pyriochou A, Kotanidou A, Dalkas G, van Eickels M, Spyroulias G, Roussos C, Papapetropoulos A, Soluble guanylyl cyclase activation by HMR-1766 (ataciguat) in cells exposed to oxidative stress, *Am J Physiol Heart Circ Physiol* 295 (2008) H1763–1771. [PubMed: 18757489]
- [80]. Pankey EA, Bhartiya M, Badejo AM Jr., Haider U, Stasch JP, Murthy SN, Nossaman BD, Kadowitz PJ, Pulmonary and systemic vasodilator responses to the soluble guanylyl cyclase

- activator, BAY 60-2770, are not dependent on endogenous nitric oxide or reduced heme, *Am J Physiol Heart Circ Physiol* 300 (2011) H792–802. [PubMed: 21217076]
- [81]. Scuseria GE, Mille MD, Jensen F, Geertsen J, The dipole moment of carbon monoxide, *J. Chem. Phys* 94 (1991) 6660–6663.
- [82]. Smyth CP, McAlpine KB, The Dipole Moment of Nitric Oxide, *J. Chem. Phys* 1 (1933) 60–61.
- [83]. Winter MB, Herzik MA Jr., Kuriyan J, Marletta MA, Tunnels modulate ligand flux in a heme nitric oxide/oxygen binding (H-NOX) domain, *Proc Natl Acad Sci U S A* 108 (2011) E881–889. [PubMed: 21997213]
- [84]. Franzen S, Spin-dependent mechanism for diatomic ligand binding to heme, *Proc Natl Acad Sci U S A* 99 (2002) 16754–16759. [PubMed: 12477933]
- [85]. Salter MD, Nienhaus K, Nienhaus GU, Dewilde S, Moens L, Pesce A, Nardini M, Bolognesi M, Olson JS, The apolar channel in *Cerebratulus lacteus* hemoglobin is the route for O₂ entry and exit, *J Biol Chem* 283 (2008) 35689–35702. [PubMed: 18840607]
- [86]. Rozza AM, Menyhard DK, Olah J, Gas Sensing by Bacterial H-NOX Proteins: An MD Study, *Molecules* 25 (2020).
- [87]. Olea C, Boon EM, Pellicena P, Kuriyan J, Marletta MA, Probing the function of heme distortion in the H-NOX family, *ACS Chem Biol* 3 (2008) 703–710. [PubMed: 19032091]
- [88]. Tran R, Boon EM, Marletta MA, Mathies RA, Resonance Raman spectra of an O₂-binding H-NOX domain reveal heme relaxation upon mutation, *Biochemistry* 48 (2009) 8568–8577. [PubMed: 19653642]
- [89]. Tran R, Weinert EE, Boon EM, Mathies RA, Marletta MA, Determinants of the Heme-CO Vibrational Modes in the H-NOX Family, *Biochemistry* 50 (2011) 6519–6530. [PubMed: 21714509]

Highlights

- Proximal ligand, heme proximal strain and distal steric hindrance govern gas binding.
- Distal hydrogen bonding enhances O₂ affinity; multiple-step binding boosts NO affinity.
- Proximal strain excludes O₂ binding from soluble guanylate cyclase (sGC).
- Multiple-step NO binding enables sGC efficient NO sensing.
- “Sliding scale rule” provides insights into ‘deactivation’ and ‘reactivation’ of sGC.

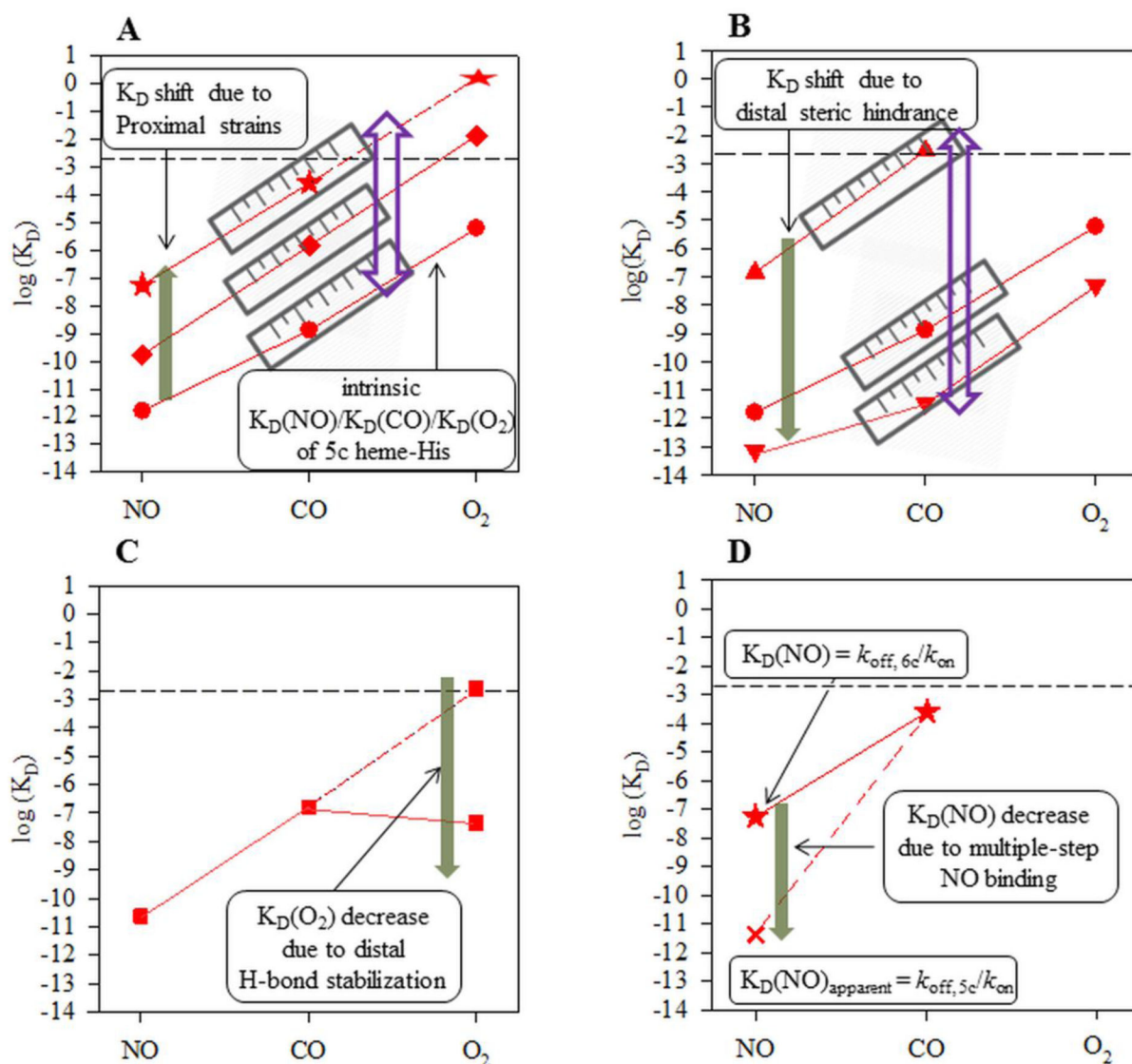


Figure 1. Major factors that govern the “sliding scale rule” hypothesis.

The “sliding scale rule” hypothesis is illustrated using binding data from sGC, two bacterial H-NOXs, Cyt *c*’, and heme model PP(1-MeIm). The logarithms of experimentally measured K_D values of hemoproteins and model compounds to NO, CO, and O_2 (red symbols) are plotted versus ligand type. Circle, PP(1-MeIm); star, sGC; up triangle, Cyt *c*’; down triangle, L16A Cyt *c*’; diamond, *Ns* H-NOX; square, *Cs* H-NOX. The horizontal dashed line in each panel represents 1atm O_2 . (A) The lines connect $\log K_D(\text{NO})$ to $\log K_D(\text{CO})$ to $\log K_D(\text{O}_2)$ of 5c heme ligated to a neutral histidine are approximately straight in both heme models and hemoproteins, due to the intrinsic binding affinity of 5c heme to the gaseous ligands. The approximate linearity of $\log K_D(\text{NO})$ - $\log K_D(\text{CO})$ - $\log K_D(\text{O}_2)$ lines is represented with a scale ruler symbol. The lines for different hemoproteins and heme models are parallel, symbolized by a sliding scale along the ordinate (purple open double-sided arrow), hence the term of “sliding scale rule”. The increased K_D s of sGC and *Ns* H-NOX compared to PP(1-MeIm) are governed by proximal strain (green solid arrow). The star connected by a red

dashed line to $\log K_D(\text{CO})$ of sGC is the predicted $\log K_D(\text{O}_2)$ of sGC. (B) Mutating distal L16 of Cyt *c'* to alanine removes distal steric hindrance, leading to large decrease in K_D s of L16A Cyt *c'* for all three gases, represented by a green solid arrow. The large range of K_D values is represented by a purple open double-sided arrow. (C) The stability of oxyferrous heme in *Cs* H-NOX is enhanced by its distal Y140 as a H-bond donor, leading to a dramatically decreased $K_D(\text{O}_2)$ (green solid arrow) but little effect on either $K_D(\text{CO})$ or $K_D(\text{NO})$. The square connected to $\log K_D(\text{CO})$ by a dashed line is the predicted $\log K_D(\text{O}_2)$ of *Cs* H-NOX by linear extrapolation of $\log K_D(\text{NO})$ - $\log K_D(\text{CO})$. (D) The conversion of 6c NO-heme complex to 5c NO-heme complex in the multiple-step NO binding of sGC and other hemoproteins leads to $K_D(\text{NO})_{\text{apparent}} \ll K_D(\text{NO})_{6c}$; the change is represented by a green solid arrow. The $\log K_D(\text{NO})_{\text{apparent}}$ is indicated by a red cross.

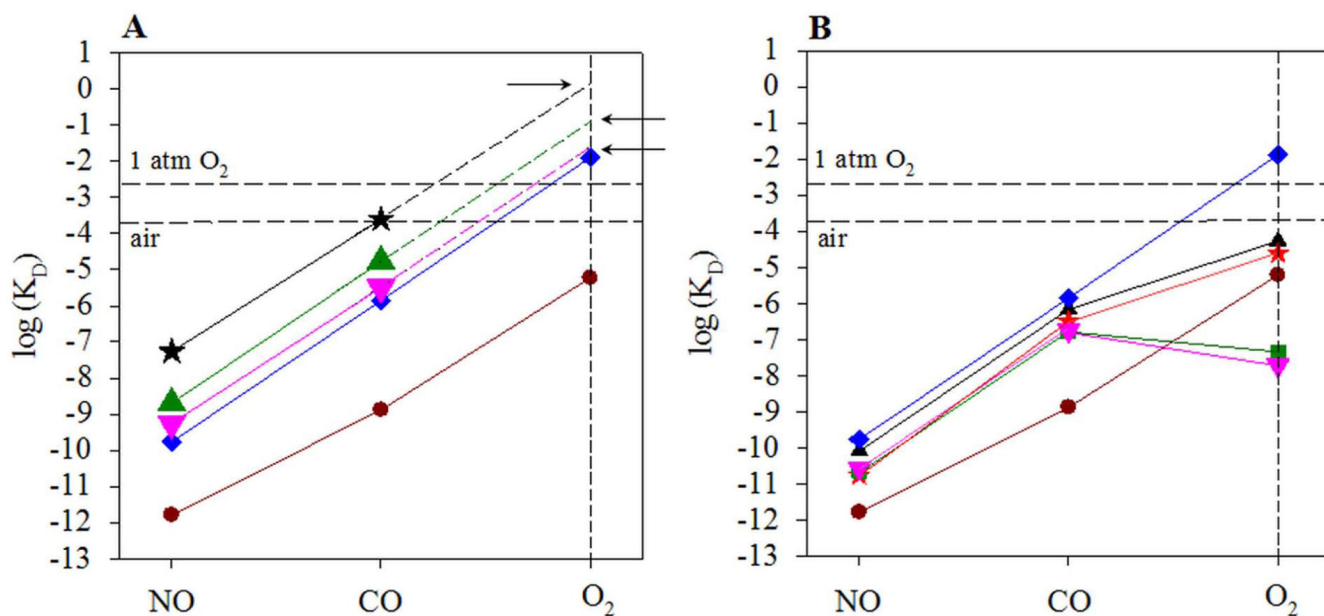


Figure 2. Gaseous ligand selectivity in truncated sGC and H-NOX proline mutants.

Logarithms of K_D s of sGC, bacterial H-NOXs, and mutants are plotted versus ligand type.

(A) black star, sGC; green up triangle, sGC $\beta_1(1-359)$, conformer 1; pink down triangle, sGC $\beta_1(1-359)$, conformer 2; blue diamond, *Ns* H-NOX; purple circle, Fe(II) PP(1-MeIm). Horizontal dashed lines, $[O_2]$ with air or 1 atm O_2 . Arrows, projected $K_D(O_2)$ s for sGC and sGC $\beta_1(1-359)$ based on the “sliding scale rule” hypothesis. (B) Black up triangle, *Cb* H-NOX; red star, P114A *Cb* H-NOX; green square, *Cs* H-NOX; pink down triangle, P115A *Cs* H-NOX. Blue diamond, *Ns* H-NOX; purple circle, Fe(II) PP(1-MeIm).

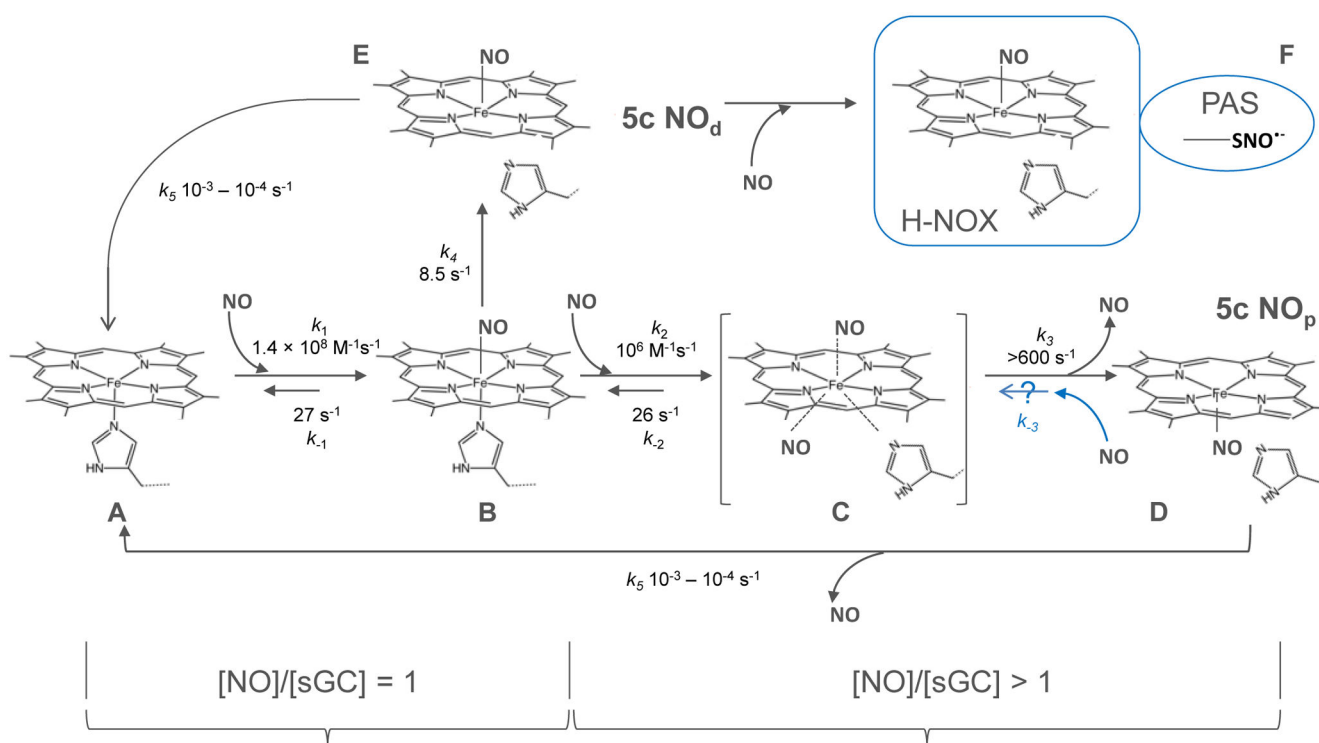


Figure 3. Multiple-step NO binding in sGC.

sGC (A) binds to NO to form a 6c NO-heme complex (B) reversibly with rate constants, $k_1 = 1.4 \times 10^8 \text{ M}^{-1}\text{s}^{-1}$ and $k_{-1} = 27 \text{ s}^{-1}$ [27]. The 6c NO-heme complex subsequently converts to a 5c NO-heme complex (E, 5c NO_d) irreversibly due to the rupture of Fe-His bond, at a rate of $k_4 = 8.5 \text{ s}^{-1}$ [27]. In the presence of excess NO, a second NO binds to B to form a transient ternary complex (C) with rate constants, $k_2 = \sim 10^6 \text{ M}^{-1}\text{s}^{-1}$ and $k_{-2} = 26 \text{ s}^{-1}$ [27]. Species C irreversibly converts to another 5c NO-heme complex (D, 5c NO_p) rapidly at a rate $> 600 \text{ s}^{-1}$ (k_3), from both Fe-His bond rupture and dissociation of distal NO. Both 5c NO_d and 5c NO_p have very small NO dissociation rate, $\sim 10^{-3} - 10^{-4} \text{ s}^{-1}$ (k_5). Reverse reaction from 5c NO_p (D) to C (k_{-3}) is assumed to happen readily in certain study but it is not supported by kinetic study (marked by a question mark) [69]. Species F, with an *S*-nitrosylthiol radical anion probably in sGC PAS domain, is proposed to be the 100% activated form in the presence of excess NO [70,73], however, this *S*-nitrosylation is unrelated to NO selectivity in sGC.

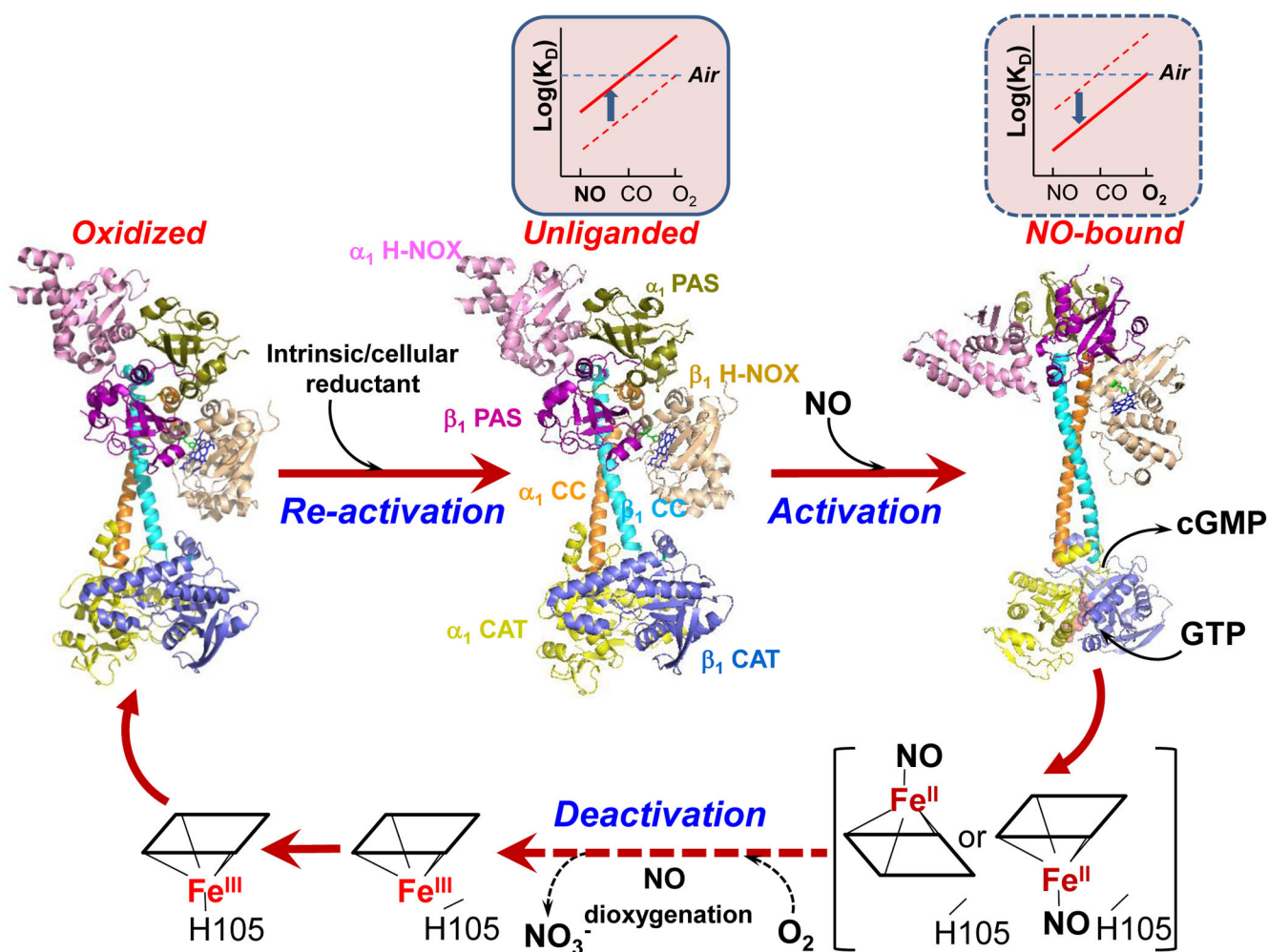


Figure 4. Possible mechanism for deactivating NO-activated sGC.

The Cryo-EM structures of sGC in different states are plotted using PyMol: oxidized state (PDB 6JT1, left), unliganded ferrous state (PDB 6JT0, middle), NO-bound activated state (PDB 6JT2, right). Domains in the three structures are marked using the same color scheme as labeled in the middle structure. Heme is represented using blue stick and His105 is represented using green stick. A molecule of phosphomethylphosphonic acid guanylate ester is bound in the NO-activated structure and is represented using spheres in salmon color. Ferrous sGC selectively binds NO, governed by strong proximal strain of heme, as shown in the “sliding scale rule” plot above the middle structure (red solid line). The rearrangement of domains in both α_1 and β_1 subunits is introduced upon NO binding which leads to His105 dissociation and a 5c NO complex (5c NO_d or 5c NO_p, represented inside the brackets under the right structure), generating an optimal binding site for GTP between α_1 and β_1 catalytic domains to produce cGMP. Dissociation of His105 releases the proximal strain of heme, which together with different domain-domain and subunit-subunit interactions due to domain rearrangement may result in high affinity for gaseous ligands. This hypothetical shift in gaseous ligand affinity is represented by the “sliding scale” plot above the right structure (red solid line), marked by a frame of broken line. Due to the increased gaseous ligand affinity, 5c NO complex may react with O₂ to generate NO₃⁻ though NO-dioxygenation and

therefore deactivates sGC (represented by the broken arrow). His105 re-associates with ferric heme iron to regenerate oxidized sGC (left structure) which can be reduced by either intrinsic or cellular reductant to its ferrous state (middle structure), ready for the next round of NO activation.

Author Manuscript

Author Manuscript

Author Manuscript

Author Manuscript